Nephrol Dial Transplant (2005) 20: 1833–1841
doi:10.1093/ndt/gfh916
Advance Access publication 14 June 2005

Nephrology Dialysis Transplantation

Original Article

Sodium retention in rats with liver cirrhosis is associated with increased renal abundance of NaCl cotransporter (NCC)

Zhenrong Yu[1], Andreas Serra[1], Daniel Sauter[2], Johannes Loffing[2], Daniel Ackermann[1], Felix J. Frey[1], Brigitte M. Frey[1] and Bruno Vogt[1]

[1]Division of Nephrology and Hypertension, University Hospital Inselspital, Berne, Switzerland and [2]Institute of Anatomy, University of Zürich, Zürich, Switzerland

Abstract

Background. Liver cirrhosis is associated with enhanced renal tubular sodium retention, the mechanism of which is still debated. We hypothesized that liver cirrhosis is associated with increased expression of renal epithelial sodium transporter(s).

Methods. Liver cirrhosis was induced by bile duct ligation (BDL) in rats. Steady state mRNA of ENaC subunits α, β, γ serum and glucocorticoid inducible kinase (Sgk1) were measured by *Taq*Man PCR in kidney homogenates at week 1, 2, 3 and 4 after BDL. Renal protein content of ENaC subunits, ubiquitin-protein-ligase Nedd4-2 and NaCl cotransporter (NCC) were assessed by western blot. Subcellular localization of ENaC subunits and NCC were analysed by immunohistochemistry.

Results. Steady state mRNA of ENaC α, β and γ were unchanged during the 4 weeks investigated, while ENaC protein decreased most prominently at week 2 (control *vs* BDL; α, −46%; β, −81%; and γ, −63%; $n=6$). Subcellular localization of ENaC subunits was not altered at week 2. Sgk1 mRNA did not change, whereas Nedd4-2 protein was reduced by >50% 2–4 weeks after BDL. NCC protein significantly increased at week 1 (control *vs* BDL: +66%, $n=6$, $P<0.05$) and decreased at week 3 (control *vs* BDL: −85%, $n=6$, $P<0.0005$).

Conclusions. Enhanced abundance of NCC was observed in the initial stage after BDL, followed by a marked decrease. ENaC transcription, translation or cell surface abundance was not increased after BDL.

Keywords: epithelial sodium channel (ENaC); bile duct ligation (BDL); liver cirrhosis; Na-Cl cotransporter (NCC); Nedd4-2; serum glucocorticoid inducible kinase 1 (Sgk1)

Introduction

Regulation of renal sodium excretion is crucial for maintaining extracellular fluid (ECF) volume within normal limits. Any manoeuvre that increases ECF volume causes a prompt and sustained natriuresis until volume returns to normal. This homeostatic mechanism is disturbed in patients with liver cirrhosis; enhanced renal salt retention increases ECF volume, contributing to the formation of oedema and ascites.

The aldosterone sensitive distal tubule (ASDN) of the kidney, comprising at least the late part of the distal convoluted tubule (DCT), the connecting tubule (CNT) and the cortical as well as the medullary collecting duct (CCD and MCD, respectively) is central for the regulation of ECF volume in many disease states [2]. With respect to liver cirrhosis, several lines of evidence suggest that the ASDN is the key segment involved in enhanced renal sodium retention and potassium loss. For example, it is well established in clinical practice that the mineralocorticoid receptor antagonist spironolactone with its primary action in the ASDN restores ECF volume in patients with liver cirrhosis [3]. From experimental studies it has become clear that various mechanisms explaining enhanced renal avidity of sodium in the cirrhotic disease state are most likely located in the ASDN. Increased concentrations of ligands accounting for enhanced mineralocorticoid receptor (MR) activation in CCD in liver cirrhosis have been reported. In some animal models and humans with cirrhosis, aldosterone levels were found to be increased and/or the access of cortisol to the MR enhanced, due to a bile acid-mediated

Correspondence and offprint requests to: Bruno Vogt, Division of Nephrology and Hypertension, Inselspital, University of Berne, Freiburgstrasse 15, 3010, Berne, Switzerland.
Email: bvogt@gmx.ch
Current address: Johannes Loffing, Department of Medicine—Unit of Anatomy, University of Fribourg, Switzerland
Z. Yu and A. Serra contributed equally to the work.

Published by Oxford University Press [2005]

inhibition of the enzyme 11β-hydroxysteroid dehydrogenase type 2 (11β-HSD2), the gate-keeper enzyme for MR activation by the glucocorticoid cortisol [4–6]. Taken together, these findings suggest that renal tubular mechanisms are responsible for sodium retention, which mainly occur at the ASDN, the site of action of mineralocorticoid hormones.

The rate-limiting factor of vectorial sodium transport induced by MR-activating ligands in the ASDN is the induction of the amiloride-sensitive sodium channel (ENaC) [2]. This channel is composed of homologous 2α, 1β and 1γ subunits. Serum glucocorticoid-inducible kinase (Sgk1) causes an increase in ENaC channels at the cell surface, is induced by aldosterone and appears to be a primary mediator of aldosterone action. ENaC clearance at the cell surface is regulated by ubiquitylation mainly through the ubiquitin-protein ligase Nedd4-2, a negative regulator of ENaC. Sgk1 phosphorylates Nedd4-2 and by this mechanism impairs the interaction between Nedd4-2 and ENaC, leading to elevated ENaC cell surface expression and increased sodium absorption [7].

The thiazide-sensitive NaCl cotransporter (NCC), which is expressed on the apical membrane of epithelial cells lining the distal convoluted tubule, is responsible for the reabsorption of at least 3% of the filtered load of sodium. Evidence for a regulatory action of the mineralocorticoid hormone aldosterone on NCC comes from several observations in whole-animal studies [8]. Enhanced MR activation might increase NCC expression and/or NCC sensitive sodium uptake and contribute to renal sodium retention in liver cirrhosis.

The aim of the present study was to investigate the impact of liver cirrhosis induced by bile duct ligation on the renal expression of ENaC, on the ENaC regulating proteins, and on NCC.

Methods

Experimental animals

Male Sprague-Dawley rats (200–220 g body wt) were maintained on standard laboratory chow and tap water with a 12 h light/dark cycle at a constant temperature and humidity. The animal work was undertaken according to the Swiss national legislation governing the use of animals and the committee on animal research at the University of Berne. We used bile duct excision to produce cirrhosis as in previous investigations [4]. All bile duct ligated animals had coarsely granular livers and portal hypertension by macroscopic inspection. Animals were allotted to bile duct excision ($n = 24$) or sham surgery ($n = 24$). After an adaptation period of 7 days, animals were anaesthetized with ketamine (75 mg/kg body weight) and xylazine (5 mg/kg body weight) administered subcutaneously and a 2 cm upper abdominal midline incision was made. In the experimental group, the bile duct was isolated and a 0.5 cm section was excised after a double ligation. In the sham group, the bowel and mesentery were manipulated and replaced. After 1, 2, 3 and 4 weeks, six animals per group were anaesthetized, kidneys removed, and immediately frozen in liquid nitrogen and stored at −80°C. Tissues were powdered with a mortar and pestle in a mixture of dry ice and acetone before being used for RNA extraction. Half of each kidney was fixed for immunohistochemistry [9].

Metabolic studies and plasma aldosterone

Plasma aldosterone concentrations were determined by a radioimmunoassay (Iodine-125 tracer, Coat-A-Count; Diagnostic Products Corporation, Los Angeles CA). Serum and urine creatinine was determined on a Hitachi 917 autoanalyser (Roche, Basel, Switzerland) according to a modified Jaffé method. Creatinine clearance was calculated by the standard formula $U_{creat} \times V_{urine} / P_{creat}$ (U_{creat}, creatinine concentration in urine; V_{urine}, volume of urine in 24 h collection; P_{creat}, plasma concentration of creatinine).

RNA extraction

Kidneys were homogenized in RNA extraction buffer using a Polytron. Total RNA was extracted according to the method of Chomczynski and Sacchi with minor modifications: the RNA pellet resulting from the first precipitation was resuspended in DEPC-treated water, and 0.1 vol of 2 M sodium acetate and 1 vol of phenol pH 4.0 were added sequentially [10]. The suspension was vortexed, centrifuged at 10 000 *g* for 20 min, and the upper phase precipitated with isopropanol at −20°C for 1 h.

Reverse transcription

Reverse transcription (RT) was performed using 2 mg of total RNA in a final volume of 20 ml. RNA was incubated with 500 ng of oligo(dT) primer at 65°C for 5 min, followed by incubation at room temperature for 15 min. Samples were then incubated with 250 mM deoxynucleotide triphosphates, 20 U of RNase-Inhibitor, and 25 U of AMV reverse transcriptase (Roche, Rotkreuz, Switzerland) in 1×buffer (50 mM Tris–HCl, 40 mM $MgCl_2$, 30 mM KCl, 1 mM DDT, pH 8.5) at 42°C for 1 h. For control reactions (RT–), enzymes were replaced by DEPC-treated-water.

Real-time PCR

Primers (Microsynth, Balgach, Switzerland) and *Taq*Man probes (Applied Biosystems, Rotkreuz, Switzerland) unique for each rat isoform were designed, optimized and validated: 5′-ctgccaagtatgatgacatcaagaa (GAPDH); 3′-agcccaggatgccctttagt (GAPDH); 5′-cagggtgatggtgcatggt (α-ENaC); 3′-ccacgccaggcctcaag (α-ENaC); 5′-cataatcctag cctgtctgtttgga (β-ENaC); 3′-cagttgccataatcagggtagaaga (β-ENaC); 5′-tgcaagcaatcctgtagctttaag (γ-ENaC); 3′-gaagcc tcagacggccatt (γ-ENaC); 5′-gagggagcgctgcttcct (Sgk1); 3′-acccaaggcactggctatttc (Sgk1). These probes were used for GAPDH (tcggccgcctgcttcacca); α-ENaC (tgaagccaccat catccataaaggcag); β-ENaC (ccctgcagtcatcggaacttcacacct); γ-ENaC (aatggacactgaccaccagcttggc); Sgk1 (ccccgtgctcgctt ctacgca). Real-time quantitative *Taq*Man PCR was performed by ABI PRISM 7700 Sequence Detection System. Diluted RT samples (10 ng of total RNA) were amplified in a final volume of 25 ml. Primers were used at a

concentration of 200 nM, probes (FAM/TAMRA labelled) at a concentration of 100 nM except for γENaC for which the probe concentration was 200 nM. GAPDH was used as a housekeeping gene and amplified in separate reactions. RT^+ reactions were performed in triplicate, RT^- in duplicate. The thermal cycling conditions were as follows: 50°C for 2 min, 95°C for 10 min, followed by 40 cycles of 95°C for 15 s and 60°C for 1 min.

Western blots

Sucrose buffer containing 250 mM sucrose, 1 mg/ml leupeptin (Sigma, St Louis, MO), 10 mM triethanolamine (Merck, Germany) and 0.1 mg/ml PMSF (Calbiochem, Germany), pH 7.6 was freshly prepared. Frozen powdered kidney tissue was homogenized in cold sucrose buffer using FastPROTEIN GREEN tubes (Lysing Matrix D, Q-Biogene, Alexis Corp, Lausanne, Switzerland) and a BIO 101 Savant FastPrep FP120 device (Q-Biogene) at a speed of 4.0 U for 20 s. The homogenized tissue was centrifuged at 4°C, 3600 r.p.m. for 10 min. The supernatant was kept on ice and the pellet, dissolved in sucrose buffer, was centrifuged at the same speed again. The second supernatant was pooled with the first supernatant and the protein concentration determined using the BCA kit (Pierce BCA Protein Assay Reagent Kit, Pierce). From each sample 30 mg of protein was incubated with Lämmli buffer at 37°C for 30 min and then immediately loaded onto 8 or 10% polyacrylamide gels. Proteins were transferred from the gels to PVDF membranes (Immobilon, Millipore Corp, Bedford, MA). Blots were blocked with 5% non-fat milk at room temperature for 90 min and incubated with the appropriate affinity-purified polyclonal antibody overnight at 4°C (see below). The secondary antibody conjugated to horseradish peroxidase was a rabbit anti-chicken/turkey IgG for βENaC (Zymed, CA, USA) protein and a swine anti-rabbit IgG (DAKO, Denmark) for αENaC, γENaC and NCC. Antibody binding was visualized by enhanced chemoluminescence (ECL; Amersham Pharmacia Biotech, UK). The densitometry of the individual bands was performed using the Scion Image software. The quantified data of western blots are expressed as arbitrary units divided by their respective GHPDA signal. GAPDH was used as loading control and remained stable over the study period [which was not the case of β-actine (results not shown)]. Affinity-purified rabbit antibody against αENaC was a gift from Dr L. Dijkink (Universiteit Nijmegen, The Netherlands), the rabbit antibody against γENaC from Dr Nicolette Farman (INSERM U478, Paris, France). The antibody against βENaC was raised in chicken using the peptide (amino acids 46–68) NH_2-CNYDSLRLQPLDTMESDSEVEAI (Davids Biotechnology, Regensburg, Germany) [11]. Nedd4-2 antibody was made by O. Staub, University of Lausanne, Switzerland [12]. NCC antibody was obtained from J. Loffing [13].

Immunohistochemistry

Kidney fixation and immunohistochemistry for ENaC were performed at weeks 1 and 2 as described [9]. For detection of ENaC, we used a set of newly generated rabbit anti-rat ENaC antibodies that were kindly provided by Dr B. Rossier, University of Lausanne, Switzerland. Serial cryosections were stained with the anti-rat αENaC antiserum diluted 1:1000, the anti-rat βENaC antiserum diluted 1/500, the anti-rat γENaC antiserum diluted 1:400, and the anti-rabbit NCC diluted 1/1000 antiserum. Binding sites of the primary antibodies were detected with Cy3-conjugated donkey anti-rabbit IgG (Jackson Immuno Research Laboratories, West Grove, PA), diluted 1/1000 [13]. All antibodies were diluted in PBS/BSA 1%. For control of unspecific antibody binding, the primary antibodies were omitted or replaced by a non-immune rabbit serum. Immunostainings were evaluated by two investigators blinded for the treatment group of the animals. Both investigators came independently to the same conclusions concerning the subcellular localization and quantitatively assessed immunostaining intensities for the analysed proteins.

Statistics

Statistical analyses were performed with SYSTAT 10.0 for Windows (SPSS INC, Chicago, IL) for non-parametric data (Mann–Whitney). Two-way ANOVA was used to determine the effect of time and treatment with BDL on measured parameters. Results are presented as mean ± SD.

Results

Metabolic studies and plasma aldosterone concentrations

At week 1, jaundice was present in the BDL animals and at week 3 these animals showed clear signs of ascite formation. Body weight increased at week 4 when compared to the sham operated animals (Table 1). Sodium retention was observed at weeks 1 and 4 with no significant reduction in renal function (Table 2). Plasma aldosterone concentrations were unchanged in BDL rats when compared to control animals at weeks 1–4 (control *vs* BDL: week 1, 482 ± 52 *vs* 416 ± 70 pM; week 2, 884 ± 188 *vs* 841 ± 191 pM; week 3, 748 ± 142 *vs* 620 ± 149 pM; week 4, 498 ± 95 *vs* 671 ± 105 pM; $n = 6$ in each group, P = NS for each week).

mRNA expression and protein amount of ENaC

Expression of α, β and γENaC mRNAs in the kidneys of BDL rats did not change throughout the 4 week study period (results not shown). Abundance of α, β and γENaC protein was decreased in BDL rats at week 1 (control *vs* BDL: α, −24 ± 11%; β, −42 ± 9%; and γ, −52 ± 12%; $n = 6$; $P < 0.001$); this decrease was more

Table 1. Body weight of control and BDL rats at weeks 0–4 before and after bile duct excisions

Body weight	Week 0	Week 1	Week 2	Week 3	Week 4
Control	221 ± 9	238 ± 9	243 ± 9	254 ± 13	259 ± 11
BDL	223 ± 8	234 ± 7	249 ± 5	252 ± 11	269 ± 14

Control *vs* BDL: weeks 0–3, P = NS; week 4, $P < 0.003$.

Table 2. Urinary Na^+ and K^+ excretion (mmol/24 h) and creatinnine clearance (ml/min per 100 g body wt) before and after bile duct excision

Values	Control	BDL			
	Week 0	Week 1	Week 2	Week 3	Week 4
Na^+ urine	0.78 (±0.5)	0.45* (±0.5)	0.62 (±0.4)	0.63 (±0.9)	0.40* (±0.6)
K^+ urine	0.19 (±0.3)	0.15 (±0.1)	0.25 (±0.6)	0.14 (±0.2)	0.21 (±0.2)
Creatinine	0.83 (±0.1)	0.5** (±0.4)	0.6 (±0.3)	0.5 (±0.7)	0.8 (±0.3)

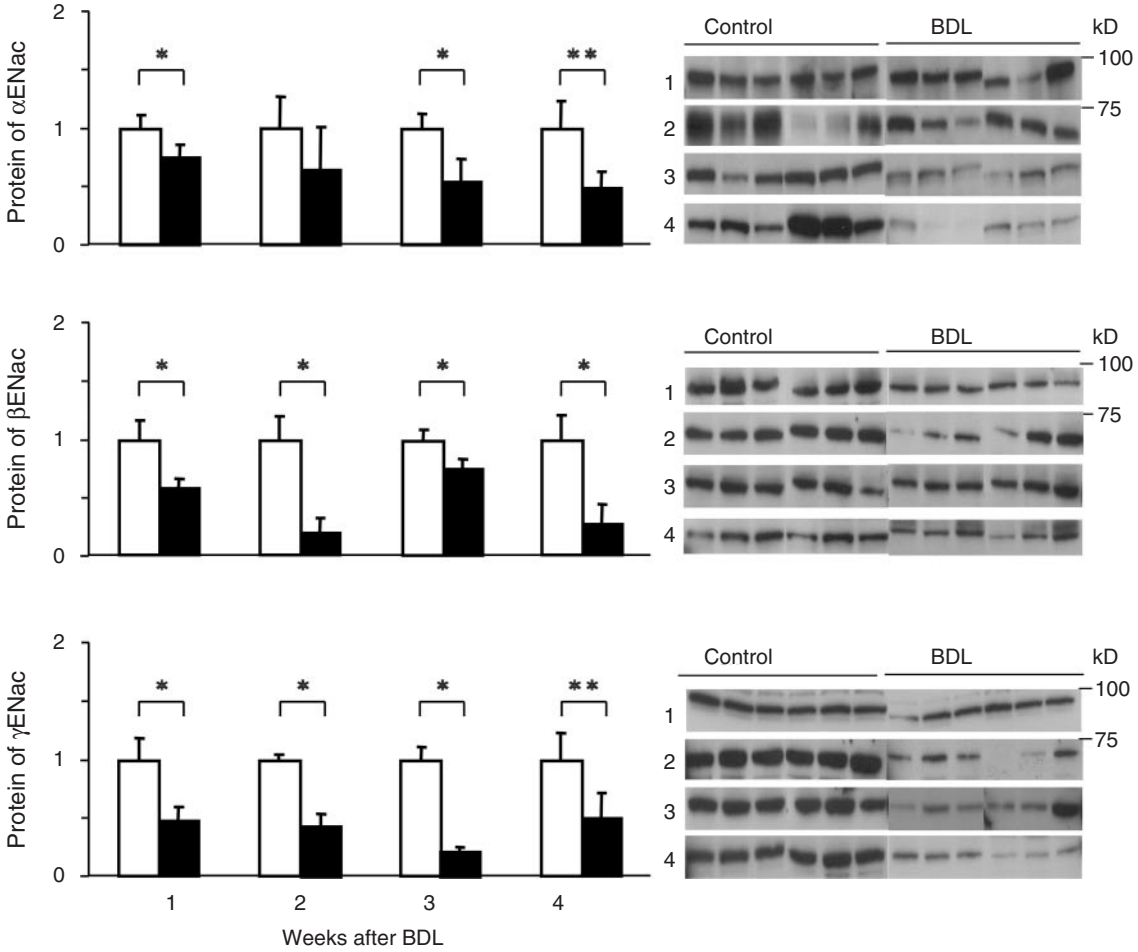

Fig. 1. Protein amount of ENaC subunits in kidneys from rats with BDL-induced liver cirrhosis (black bars) and control animals (open bars) as assessed by quantitative western blot. For each time point, $n=6$ BDL rats were compared with $n=6$ sham-operated animals. Values are mean ± SD; *$P<0.005$ and **$P<0.01$.

pronounced at week 2 (control *vs* BDL: α, −46 ± 42%; β, −81 ± 13%; and γ, −63 ± 18%; $n=6$; $P<0.001$) and at week 4 (control *vs* BDL: α, −51 ± 20%; β, −73 ± 18%; and γ, −55 ± 20%; $n=6$; $P<0.001$) (Figure 1). ANOVA analysis for αENaC protein revealed no difference between the BDL groups at different time points, for βENaC BDL the group from week 2 was different when compared to week 1 ($F=9.814$; $P<0.0035$), but not different to BDL at week 4. For γENaC, BDL of week 3 is more decreased compared to week 1 ($F=9.705$; $P<0.004$).

Sgk1 and NCC mRNA expression. Protein amount of Nedd4-2 and NCC

Steady state levels of Sgk1 mRNA were not different in BDL rats and in sham operated animals (results not shown). Nedd4-2 protein content decreased during the study period with the most prominent decline at week 2 (control *vs* BDL: −65 ± 22%, $n=6$; $P<0.001$) (Figure 2). The abundance of NCC was significantly increased in BDL compared to control at week 1 (control *vs* BDL: +66 ± 41%, $n=6$; $P<0.05$) and

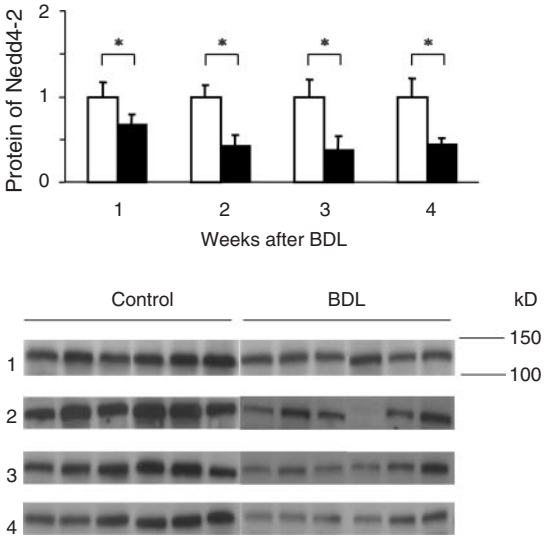

Fig. 2. Protein amount of Nedd4-2 in kidneys from rats with BDL-induced liver cirrhosis (black bars) and control animals (open bars) as assessed by quantitative western blot. For each time point, $n = 6$ BDL rats were compared with $n = 6$ sham-operated animals. Values are mean ± SD; $^*P < 0.005$.

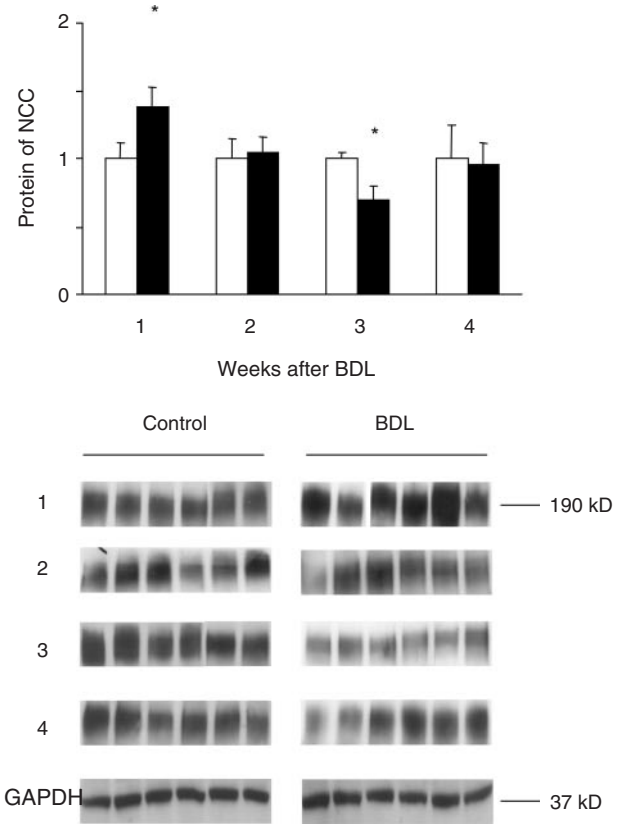

Fig. 3. Protein amount of NCC in kidneys from rats with BDL-induced liver cirrhosis (black bars) and control animals (open bars) as assessed by quantitative western blot. For each time point, $n = 6$ BDL rats were compared with $n = 6$ sham-operated animals. Values are mean ± SD; $^*P < 0.05$.

decreased in BDL at week 3 when compared to control (control *vs* BDL: −85% ± 20%, $n = 6$; $P < 0.0005$; Figure 3), without changes in mRNA expression except an increase at week 4. No difference was detected between BDL and control at weeks 2 and 4. ANOVA analysis revealed a difference between BDL week 1 to week 2 ($F = 9.934$; $P < 0.003$) and between week 1 and weeks 3 and 4, respectively ($F = 9.705$; $P < 0.004$).

Immunohistochemistry of ENaC and NCC

The cellular and subcellular localization of α, β and γENaC subunits and NCC were analysed in the kidney cortex of sham operated and BDL rats at week 1 and at week 2 after surgery (four rats in each group). The time point after surgery had no effect on the immunostaining for ENaC subunits. Therefore, results are shown only for week 2 (Figures 4–6). In sham operated rats, the antibody binding pattern for α, β and γENaC subunits and NCC were comparable to those described previously in normal rats. As shown exemplarily for βENaC in Figure 4, ENaC was detectable in CNT and CCD profiles grouped around the cortical radial vessels or running in the medullary rays, respectively. The analysis of the renal tissue obtained from sham operated and BDL revealed similar ENaC distribution. However, βENaC and γENaC (not shown) immunostaining in the CCDs, but not CNTs, were weaker in BDL than in sham operated rats. Higher magnification of the CNT and CCD profiles (Figures 5 and 6) reveal for all groups a predominant intracellular localization of ENaC subunits in the CNT and CCD cells. Only for αENaC was occasionally a weak apical immunostaining observed in some CNT profiles (Figure 5). NCC was detected in DCT profiles located in the renal cortex of sham operated and BDL rats. Consistent with the western blot data, NCC-related immunostaining was more pronounced in DCTs of BDL than of sham operated rats at week 1, but not at week 2 (Figure 7).

Discussion

Ascites and oedema formation in liver cirrhosis induced by BDL in rats is due to increased renal sodium reabsorption. The present study was designed to investigate ENaC, the ENaC regulatory proteins Sgk1 and Nedd4-2, and NCC in BDL rats. Following BDL, (i) mRNA of ENaC subunits remain stable, (ii) protein amounts of α, β and γENaC decreases, (iii) mRNA of Sgk1 is unchanged, (iv) subcellular distribution of ENaC subunits is not altered when analysed by immunohistochemistry despite decreased expression of Nedd4-2 protein, and (v) protein abundance of NCC increases at week 1 when analysed by immunoblotting and immunohistochemistry.

The protein amount of α, β and γENaC was decreased in BDL rats despite stable mRNA expression of the corresponding ENaC subunits (Figure 1).

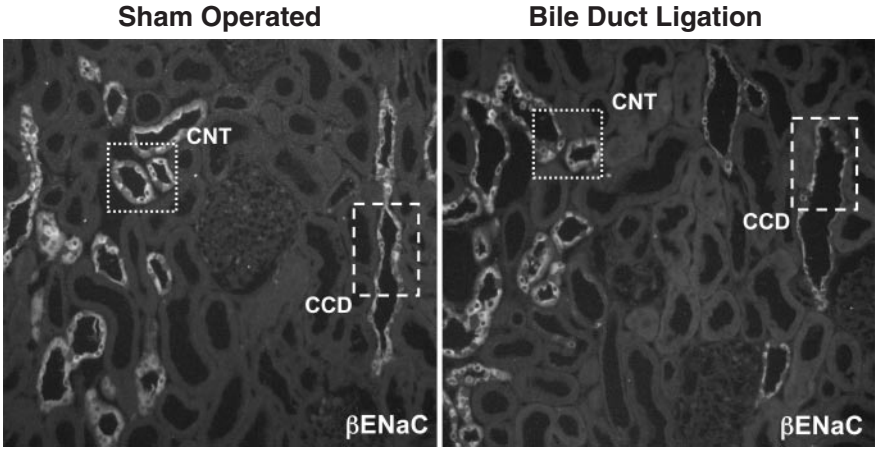

Fig. 4. Immunohistochemical detection of βENaC in the renal cortex of a sham-operated rat (left panel) and a BDL rat (right panel) at week 2; boxes, connecting tubule (CNT) and cortical collecting duct (CCD) profiles shown at higher magnification in Figures 5 and 6, respectively.

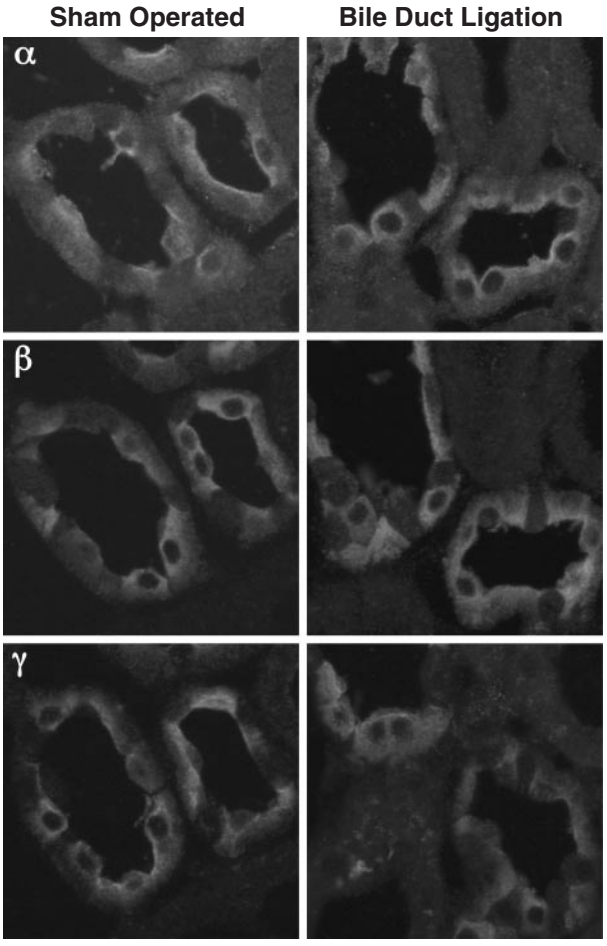

Fig. 5. Immunohistochemical detection of α, β and γENaC in consecutive CNT profiles of a sham-operated rat (left panel) and a BDL rat (right panel); consecutive cryosections immunostained with rabbit-anti-rat α, β and γENaC antibodies followed by a Cy3-conjugated goat-anti-rabbit IgG. ENaC subunits are diffusely distributed throughout the cytoplasm of a subset of CNT cells. Only αENaC is occasionally observed at the apical plasma membrane of CNT cells. Unstained cells in CNT profiles represent intercalated cells.

Thus, it is not possible to link directly the amount of ENaC protein with transcription. Berger *et al.* [14] studied the relevance of the MR on mRNA abundance of ENaC by using MR knockout mice. MR deficiency did not affect the mRNA abundance of α, β and γENaC subunits in the kidney of MR–/–mice, indicating that MR-mediated control of renal Na^+ reabsorption was not achieved by transcriptional control of ENaC expression [14]. Recent investigations by Escoubet *et al.* [15] revealed that aldosterone depletion had no or only a weak effect on renal α, β and γENaC subunits mRNA expression. Our results of decreased amounts of α, β and γENaC despite enhanced MR activation by 11b-hydroxy-steroids in BDL rats are in line with these observations suggesting the absence of a direct link between MR activation and mRNA and protein levels of ENaC subunits. Thus, other as yet unidentified mechanisms are involved in the regulation of α, β and γENaC in health and disease states [14,15].

We measured the total amount of ENaC protein by quantitative western blot. It is conceivable that the pattern of intracellular distribution of ENaC subunits is altered in the BDL-induced disease state, an effect that would have been missed by these analyses. An altered pattern of ENaC distribution might be attributable to a post-transcriptional regulatory event, either by affecting biosynthesis or stability of the ENaC proteins.

Two proteins are interesting with respect to the regulation of ENaC: Nedd4-2, which negatively controls cell surface density of ENaC, and Sgk1, which is an aldosterone-dependent, positive regulator of ENaC expression [7,16]. Nedd4-2 protein amount was decreased in weeks 1–4 in BDL rats when compared to sham operated animals (Figure 2). Based on the role of Nedd4-2, one might predict an increased abundance of ENaC protein in rats with BDL, which is definitely not the case (Figure 1). In the present study we assessed the total amount of Nedd4-2. Thus it is still conceivable that the amount of biologically active

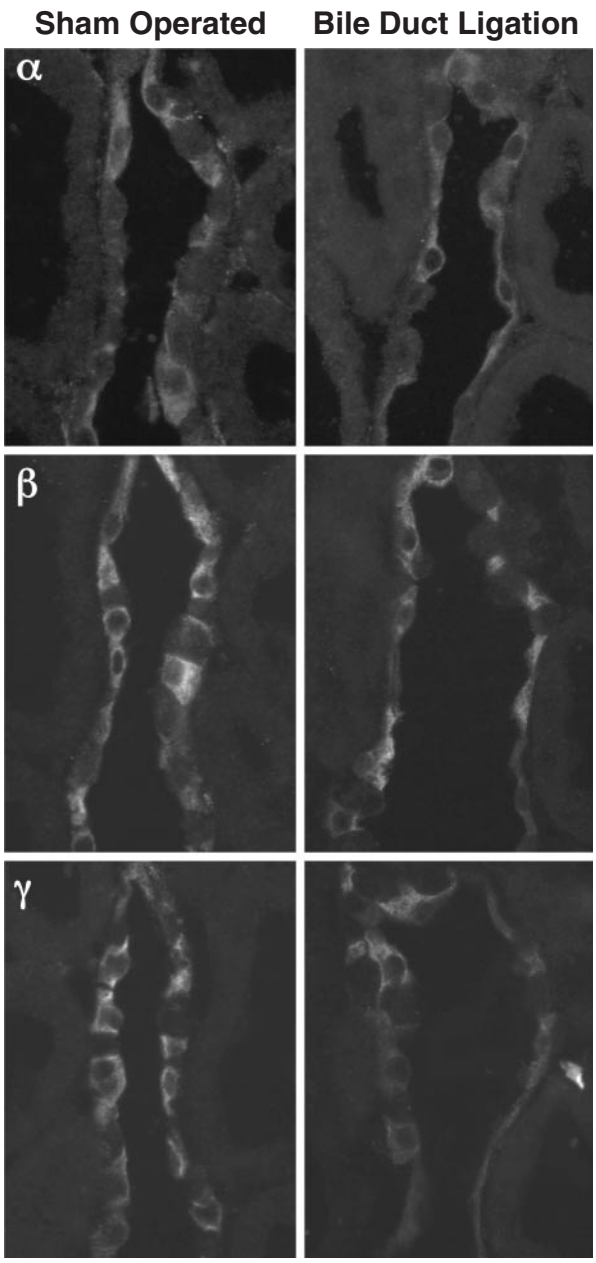

Fig. 6. Immunohistochemical detection of α, β and γENaC in consecutive CCD profiles of a sham operated rat (left panel) and a BDL rat (right panel); consecutive cryosections immunostained with rabbit-anti-rat α, β and γENaC antibodies followed by a Cy3-conjugated goat-anti-rabbit IgG. ENaC subunits are diffusely distributed throughout the cytoplasm of a subset of CCD cells. Unstained cells in CNT profiles represent intercalated cells.

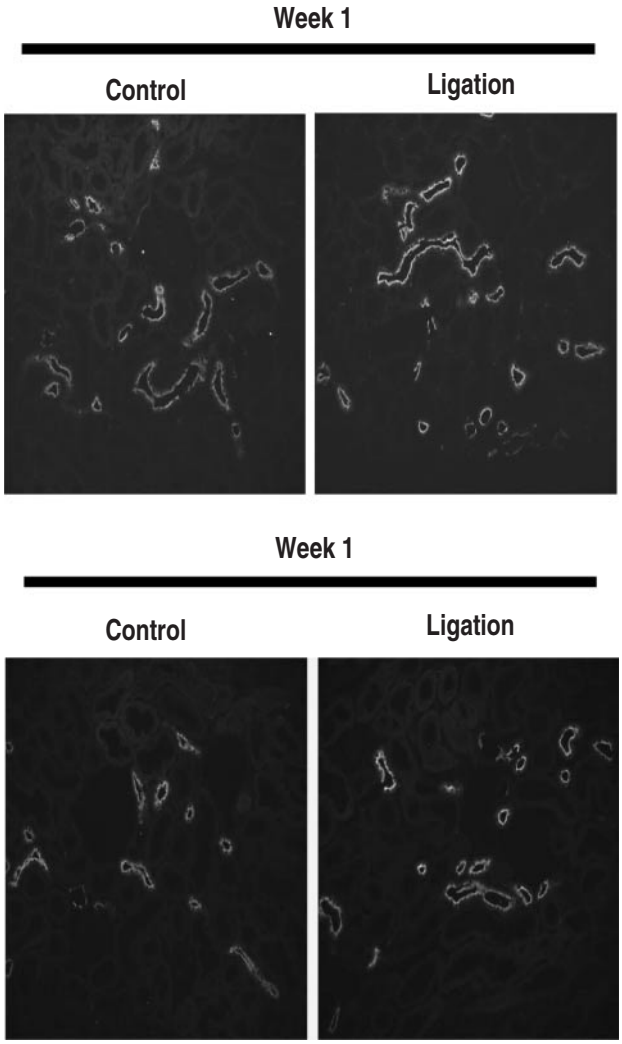

Fig. 7. Immunohistochemical detection of NCC in DCT profiles, sham-operated rats (left column) and BDL rats (right column) at week 1 (upper row), and week 2 (lower row); cryosections immunostained by rabbit-anti-rat βENaC antibody followed by a Cy3-conjugated goat-anti-rabbit IgG. NCC is exclusively seen in DCT located in the renal cortex. BDL slightly increases NCC-related immunostaining in week 1, but not in week 2, when compared to the respective sham-operated control.

unphosphorylated Nedd4-2 was unchanged in BDL rats and therefore ENaC did not change. Alternatively, Nedd4-2 might have changed in kidney segments not expressing ENaC, thus concealing a direct link between Nedd4-2 and ENaC levels. Nedd4-2 simply affects intracellular localization of ENaC and not the total pool. To assess the effect of the observed down-regulation of Nedd4-2 on the intracellular localization of ENaC, we performed an immunohistochemical analysis of all three ENaC subunits. Subcellular distribution of all three subunits was not disturbed in BDL animals when compared to the appropriate controls, indicating that Nedd4-2 downregulation appears to exhibit no or only a minor effect on intracellular localization of ENaC in this specific disease state (Figures 4–6). An unexplained finding is the slight, but steadily decreasing protein abundance of Nedd4-2 in the controls (Figure 2). mRNA of Sgk1 is present in BDL rats; however, no modulation of Sgk1 expression assessed by steady-state mRNA measurements was observed.

We measured α, β and γENaC mRNA and protein in BDL rats but did not assess ENaC activity in the CCD. One might speculate that ENaC is activated despite the presence of normal or low amounts of ENaC proteins. Such an activation might occur through increased bile acid concentrations in BDL

rats. Lima *et al.* [17] have shown that the bile acid deoxycholate stimulates the amiloride sensitive sodium current in frog skin. However, until the activity of ENaC is not measured directly by electrophysiological methods in the renal tubular segments from BDL rats such a mechanism remains speculative.

Jonassen *et al.* [18] proposed the thick ascending limb (TAL) and not the CCD to be responsible for abnormal renal sodium retention in BDL rats. They measured Na,K-ATPase activity at V_{max} conditions in microdissected tubules from TAL and outer medullary collecting duct (OMCD) in rats 5 weeks after BDL. Na,K-ATPase activity per mm tubule length was decreased in the OMCD and unchanged in the TAL. This interesting finding is not at variance with our study because the authors considered the OMCD and not CCD and, furthermore, the measurements took place at a relatively late time point after BDL (week 5) when the mineralocorticoid escape phenomenon is present. In addition, it has been suggested that measurement of Na,K-ATPase at V_{max} and not at lower V might jeopardize the identification of dysregulations of the Na,K-ATPase activity in disease states.

The NCC located in the apical membrane of the DCT is responsible for the thiazide-sensitive sodium uptake. Expression of NCC was increased 1 week after BDL with stronger immunostaining for NCC in the DCTs when compared to control (Figures 3 and 7). NCC mediated sodium uptake is stimulated by forskolin, a drug that promotes the adenylyl cyclase-catalyzed production of cAMP, acting through PKA. However, PKA-induced sodium uptake by activation of NCC does not increase expression of NCC and therefore might not account for the mechanism of increased NCC in BDL rats. In the long term, aldosterone causes a significant increase in protein amount of NCC and in NCC mediated sodium uptake. This mechanism seems unlikely because the plasma aldosterone concentration was similar in BDL animals when compared to the control animals. An aldosterone-independent activation of MR has been identified in rats with BDL and in human subjects with elevated serum bile acids might represent a possible pathway to activate NCC in the cirrhotic disease state.

An unexplained finding is the strong decrease in NCC protein amount 3 weeks after BDL. A similar observation was reported by Fernandez-Llama *et al.* [19] in a model of liver cirrhosis secondary to chronic CCl_4 inhalation. The authors measured a decrease in renal NCC protein at weeks 12–25 after starting cirrhosis induction with CCl_4. One might speculate if this decreased NCC protein amount in BDL rats at 3 weeks and in the chronic cirrhosis model induced by CCl_4 inhalation is not simply representing a mineralocorticoid escape phenomenon known to decrease substantially the NCC protein amount in the kidney [19]. In a recent publication from Fernandez-Llama *et al.* an increase in NCC protein and αENaC was observed in the same liver cirrhosis model induced by CCl_4 inhalation. The authors relate these changes to an aldosterone effect. The discrepancy of the different observations is probably related to the different time point of observation, and with regard to our study, to the different animal model [20].

In conclusion, the expression of NCC is increased in kidney homogenates 1 week after BDL, a finding that might explain early renal sodium retention in BDL induced liver disease. The expression of α, β and γENaC subunits is decreased in kidney tissue of BDL rats without evidence for changes in subcellular distribution of the three ENaC subunits.

Acknowledgements. We thank L. Dijkink for αENaC antibody, Nicolette Fareman for γENaC antibody, Olivier Staub for Nedd4-2 antibody, Bernard Rosser for α, β and γ antibodies, and Beatrice Rohrbach for technical assistance. This work was supported by two grants from the Swiss National Foundation for Scientific Research (Nr 32-57205.99).

Conflict of interest statement. None declared.

References

1. Arroyo V, Bernardi M, Epstein M, Henriksen JH, Schrier RW, Rodes J. Pathophysiology of ascites and functional renal failure in cirrhosis. *J Hepatol* 1988; 6: 239–257
2. Meneton P, Loffing J, Warnock DG. Sodium and potassium handling by the aldosterone-sensitive distal nephron: the pivotal role of the distal and connecting tubule. *Am J Physiol Renal Physiol* 2004; 287: F593–F601
3. Gregory PB, Broekelschen PH, Hill MD, Lipton AB, Knauer CM, Egger M *et al.* Complications of diuresis in the alcoholic patient with ascites: a controlled trial. *Gastroenterology* 1977; 73: 534–538
4. Ackermann D, Vogt B, Escher G, Dick B, Reichen J, Frey BM *et al.* Inhibition of 11beta-hydroxysteroid dehydrogenase by bile acids in rats with cirrhosis. *Hepatology* 1999; 30: 623–629
5. Quattropani C, Vogt B, Odermatt A, Dick B, Frey BM, Frey FJ. Reduced activity of 11 beta-hydroxysteroid dehydrogenase in patients with cholestasis. *J Clin Invest* 2001; 108: 1299–1305
6. Jimenez W, Martinez-Pardo A, Arroyo V, Bruix J, Rimola A, Gaya J *et al.* Temporal relationship between hyperaldosteronism, sodium retention and ascites formation in rats with experimental cirrhosis. *Hepatology* 1985; 5: 245–250
7. Kamynina E, Staub O. Concerted action of ENaC, Nedd4-2, and Sgk1 in transepithelial Na(+) transport. *Am J Physiol Renal Physiol* 2002; 283: F377–F387
8. Kim GH, Masilamani S, Turner R, Mitchell C, Wade JB, Knepper MA. The thiazide-sensitive Na-Cl cotransporter is an aldosterone-induced protein. *Proc Natl Acad Sci USA* 1998; 95: 14552–14557
9. Loffing J, Zecevic M, Feraille E, Kaissling B, Asher C, Rossier BC *et al.* Aldosterone induces rapid apical translocation of ENaC in early portion of renal collecting system: possible role of SGK. *Am J Physiol Renal Physiol* 2001; 280: F675–F682
10. Chomczynski P, Sacchi N. Single-step method of RNA isolation by acid guanidinium thiocyanate-phenol-chloroform extraction. *Anal Biochem* 1987; 162: 156–159
11. Masilamani S, Kim GH, Mitchell C, Wade JB, Knepper MA. Aldosterone-mediated regulation of ENaC alpha, beta, and gamma subunit proteins in rat kidney. *J Clin Invest* 1999; 104: R19–R23
12. Kamynina E, Tauxe C, Staub O. Distinct characteristics of two human Nedd4 proteins with respect to epithelial Na(+)

channel regulation. *Am J Physiol Renal Physiol* 2001; 281: F469–F477
13. Nijenhuis T, Hoenderop JG, Loffing J, van der Kemp AW, van Os CH, Bindels RJ. Thiazide-induced hypocalciuria is accompanied by a decreased expression of Ca2+ transport proteins in kidney. *Kidney Int* 2003; 64: 555–564
14. Berger S, Bleich M, Schmid W, Cole TJ, Peters J, Watanabe H *et al*. Mineralocorticoid receptor knockout mice: pathophysiology of Na+ metabolism. *Proc Natl Acad Sci USA* 1998; 95: 9424–9429
15. Escoubet B, Coureau C, Bonvalet JP, Farman N. Noncoordinate regulation of epithelial Na channel and Na pump subunit mRNAs in kidney and colon by aldosterone. *Am J Physiol* 1997; 272: C1482–C1491
16. Chen SY, Bhargava A, Mastroberardino L, Meijer OC, Wang J, Buse P *et al*. Epithelial sodium channel regulated by aldosterone-induced protein sgk. *Proc Natl Acad Sci USA* 1999; 96: 2514–2519
17. Lima MS, Ferreira HG, Ferreira KT. The effect of bile acid on the activation of amiloride-sensitive sodium channels in frog skin. *Exp Physiol* 1996; 81: 755–766
18. Jonassen TE, Heide AM, Janjua NR, Christensen S. Collecting duct function in liver cirrhotic rats with early sodium retention. *Acta Physiol Scand* 2002; 175: 237–244
19. Fernandez-Llama P, Jimenez W, Bosch-Marce M, Arroyo V, Nielsen S, Knepper MA. Dysregulation of renal aquaporins and Na-Cl cotransporter in CCl4-induced cirrhosis. *Kidney Int* 2000; 58: 216–228
20. Fernandez-Llama P, Ageloff S, Fernandez-Varo G, Ros J, Wang X, Garra N *et al*. Sodium retention in cirrhotic rats is associated with increased renal abundance of sodium transporter proteins. *Kidney Int* 2005; 67: 622–630

Received for publication: 28.7.04
Accepted in revised form: 22.4.05